

The synthesis and spectral characterization of copper sulfide nanofluid in a spectral splitting PV/T system

Zhang Jie^{ab*}, Salina Muhamad^a, Izyani Mat Rusni^a, Yang Xiping^b, Kuang Xin^b

^aFaculty of Engineering and Life Sciences, Universiti Selangor, 45600 Bestari jaya, Selangor, Malaysia

^bJiangsu Shipping College, Nantong 226010, China

*Corresponding author. Tel.: +8618362156969; e-mail: cxcyds888@163.com

Received 23 March 2025, Revised 1 August 2025, Accepted 11 September 2025

ABSTRACT

The medium utilized in spectral splitting photovoltaic/thermal (PV/T) systems holds immense significance. Previously employed nanofluids, such as polypyrrole, Ag, ZnO, and MgO, exhibited insufficient absorption in the infrared range, hindering the photothermal units from achieving higher temperatures. Copper sulfide (CuS) emerges as a promising alternative nanofluid in PV/T systems due to its superior thermal conductivity and adjustable spectral radiation properties. To assess its suitability, four samples of CuS nanofluid are synthesized under four different oil bathing temperatures, which are 25 °C, 40 °C, 60 °C, and 80 °C, respectively. What is more, an in-depth examination of CuS nanofluid's optical characteristics and performance is conducted. The U-4100 Spectrophotometer was employed to measure its transmittance, while the Nicolet iS50 was employed to measure its reflectivity. The findings revealed that a 10 mm layer of CuS nanofluid synthesized under 80 °C oil bathing temperature possesses distinct selective absorption properties compared to the other three samples of CuS nanofluids. For this CuS nanofluid with the concentration of 100 ug/ml, the transmittance at the wavelength of 600 nm can hit 65 %, while the transmittance in the near-infrared wavelength band is lower than 16 %. These unique optical attributes underscore the potential for CuS nanofluid to be widely adopted in spectral splitting PV/T systems.

Keywords: copper sulfide nanofluid; synthesis; spectral characterization; spectral splitting; PV/T

1. INTRODUCTION

Concentrating spectral splitting photovoltaic/thermal (PV/T) systems offer a promising approach for maximizing solar energy utilization by simultaneously harvesting electricity and heat from sunlight. These systems integrate spectrally selective optical elements to split the solar spectrum, directing different wavelength bands to distinct photovoltaic and thermal absorbers. By efficiently utilizing both photovoltaic and thermal energy conversion mechanisms, concentrating spectral splitting PV/T systems have the potential to achieve higher overall energy conversion efficiencies compared to traditional photovoltaic or photothermal systems [1].

In recent years, the integration of nanofluids into PV/T systems has emerged as a promising strategy for enhancing thermal performance and overall system efficiency. Nanofluids, which are engineered colloidal suspensions of nanoparticles in a base fluid, offer unique thermal properties such as high thermal conductivity and enhanced heat transfer characteristics. Existing spectral splitting fluids have limitations in spectrum coverage and selective absorption and reflection [2-4]. Take the monocrystalline silicon cell as an example; the radiation characteristics requirement of spectral splitting fluid is shown in Fig. 1 [5]. Many fluids can only effectively absorb or reflect specific wavelengths of light, failing to cover the

entire solar spectrum, which leads to partial solar energy being wasted and reduces the overall efficiency of PV/T systems [6-9]. Additionally, these fluids lack high selective absorption and reflection properties, making it difficult to effectively direct different wavelengths of light to the respective photovoltaic and thermal conversion components, thereby affecting spectral splitting efficiency and energy conversion performance [10-11]. Integrating nanofluids into spectral splitting PV/T systems may pose challenges in terms of optical compatibility. The presence of nanoparticles can alter the optical properties of the fluid, affecting its interaction with spectral splitting elements and overall system performance. Some of the nanofluids that have been used in PV/T system are polypyrrole [12-13], Ag [14], ZnO [15-16] and MgO [17-18]. However, the main problem is unsolved. Polypyrrole is prone to oxidative degradation under prolonged illumination, leading to deterioration of its optical properties. As a noble metal material, silver nanoparticles exhibit poor economic feasibility for large-scale applications. Zinc oxide undergoes photocatalytic decomposition under light exposure and humid conditions, compromising its long-term stability. Magnesium oxide demonstrates weak energy absorption capability in the near-infrared spectral region.

In 2021, Majumdar reported copper sulfides (CuS) have been recognized as industrially significant materials with

diverse applications in exotic technological fields of photovoltaics and energy storage^[19]. CuS nanomaterials exhibit significant advantages in the field of full-spectrum solar energy utilization due to their unique photothermal conversion properties, spectrally selective absorption, and excellent stability. The efficient infrared absorption and high visible-light transmittance make them an ideal spectral splitting medium for spectral splitting PV/T systems, synergistically enhancing both photothermal conversion efficiency and photovoltaic cell performance. Moreover, CuS nanofluids offer additional benefits such as low cost, high chemical stability, and tunable dispersibility, enabling flexible adaptation to various spectral splitting requirements. These characteristics provide new insights for the design and optimization of PV/T systems, demonstrating great potential to advance the development of high-efficiency full-spectrum solar utilization technologies. Therefore, this study is conducted to synthesize the suitable CuS nanofluid for spectral splitting that can achieve better efficiency.

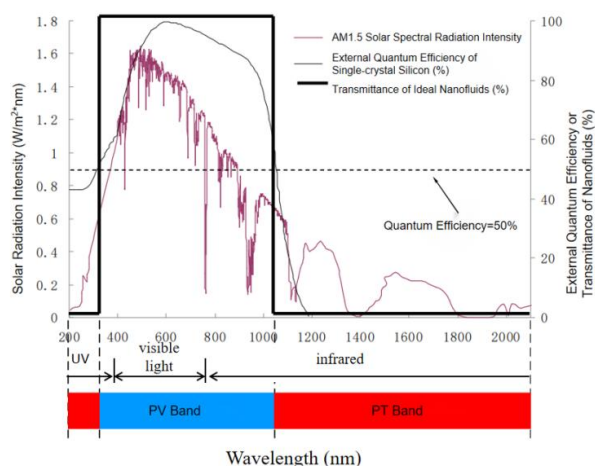


Figure 1. Radiation characteristics requirement of spectral splitting fluid (take the monocrystalline silicon cell as an example)

2. METHODOLOGY

2.1. Preparation of CuS nanofluid

The synthesis step of CuS nanofluid is as follows: 0.48 g of sodium sulfide nonahydrate and 0.34 g of copper(II) chloride dihydrate were weighed and each dissolved in 2 mL of deionized water. A round-bottom flask was prepared by adding 16 mL of deionized water and 500 mg of polyvinylpyrrolidone. Under continuous stirring, the copper chloride solution and sodium sulfide solution were sequentially added to the flask. After 20 minutes of reaction, the liquid was extracted and purified using an ultrafiltration tube. The purified liquid was then redispersed in 5 mL of deionized water to obtain Sample 1. The concentration is 50 $\mu\text{g/ml}$. When the purified liquid was then redispersed in 5 mL of deionized water, the purified liquid was then redispersed in 5 mL of deionized water. In order to inspect the effect of the reaction temperature on the performance of the CuS nanofluid, the mixture was heated in an oil bath at different

temperature^[20]. When the oil bath temperature is 40 $^{\circ}\text{C}$, sample 2 can be obtained. When the oil bath temperature is 60 $^{\circ}\text{C}$, the sample 3 can be obtained. When the oil bath temperature is 80 $^{\circ}\text{C}$, the sample 4 can be obtained. For each sample, three different concentrations were prepared, which are respectively 50 $\mu\text{g/ml}$, 100 $\mu\text{g/ml}$ and 150 $\mu\text{g/ml}$.

2.2. Measurement of Optical Properties

As shown in figure 2(a), Talos F200X G2 TEM is used to observe the microstructure of CuS nanoparticles. For TEM analysis, the CuS nanoparticle aqueous suspension was deposited onto 300-mesh copper grids coated with ultrathin carbon films and subsequently dried under atmospheric conditions before microscopic examination.

As shown in figure 2(b), the DX-2700 X-ray Diffractometer was used to measure the crystal structure of the CuS nanoparticle. The XRD characterization was conducted using Cu $K\alpha$ radiation ($\lambda = 1.5406 \text{ \AA}$) operated at 40 kV and 30 mA. The diffraction patterns were collected over a 2θ range of 10-80 $^{\circ}$ with a scanning rate of 5 $^{\circ}/\text{min}$ and a step size of 0.02 $^{\circ}$, employing a divergence slit of 1 $^{\circ}$ and a receiving slit of 0.3 mm. For sample preparation, the nanofluid was drop-cast onto a glass substrate and dried at ambient temperature to form a thin film prior to measurement. All measurements were performed under controlled room temperature conditions ($25 \pm 2 \text{ }^{\circ}\text{C}$).

As shown in figure 2(c), the transmittance of the CuS nanofluid was characterized using a U-4100 spectrophotometer equipped with a 60 mm integrating sphere. Measurements were conducted under ambient conditions ($25 \pm 2 \text{ }^{\circ}\text{C}$) over a spectral range of 200-2000 nm with a resolution of 2 nm. The nanofluid samples were loaded into quartz cuvettes with a 10 mm optical path length, using deionized water as the reference blank. Prior to measurements, the samples were homogenized via ultrasonication for 15 minutes to ensure dispersion stability. All measurements were performed with a normal incident light beam, and three consecutive scans were averaged for each sample to enhance the signal-to-noise ratio. Special attention was paid to prevent bubble formation during sample loading, and baseline correction was systematically performed before each measurement session.

As shown in figure 2(d), the reflectivity of CuS nanofluids was characterized using a Nicolet iS50 spectrometer equipped with a variable-angle reflectance accessory. Measurements were conducted at a fixed incidence angle of 8 $^{\circ}$ across the spectral range of 200-2000 nm. Prior to testing, the nanofluid samples were ultrasonically treated (40 kHz, 15 min) and vacuum-degassed before being loaded into quartz cuvettes with a 10 mm optical path length. A high-purity gold-coated mirror (reflectance >98 %) served as the reference standard. Each spectral acquisition consisted of 64 co-added scans performed at a scanning speed of 0.2 cm/s with a 100 μm aperture setting. Strict environmental controls were

maintained throughout the measurements, including precise temperature regulation (25 ± 0.1 °C), continuous nitrogen purging (5 L/min), and constant magnetic stirring (300 rpm) to ensure sample stability and measurement reproducibility.



Figure 2 Measurement instruments

3. RESULT AND DISCUSSIONS

3.1. The Characterization of the CuS

Figure 3 shows a physical image of sample 1, sample 2, sample 3, and sample 4 of CuS nanofluid with three different concentrations. It can find that the color of sample 1 and the color of sample 2 are similar, while the color of sample 3 and the color of sample 4 are similar.

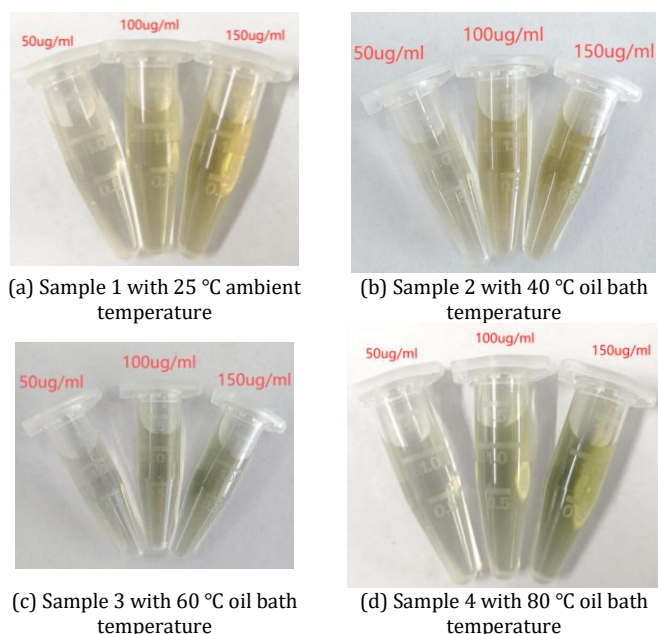


Figure 3 The four samples of CuS nanofluid with different concentrations

The prepared CuS nanofluid was characterized using Talos F200X G2 TEM. Figure 4 to figure 7 shows the images of four samples of CuS nanoparticles. CuS nanoparticles can be well dispersed in the base fluid. The TEM images of Sample 3 CuS nanoparticles and Sample 4 CuS nanoparticles show that the two CuS nanoparticles have similar nanodot structures. The average particle size of sample 1 and sample 2 CuS nanoparticles is lower than 5 nm. The TEM images of Sample 3 CuS nanoparticles and Sample 4 CuS nanoparticles show that the two CuS nanoparticles have similar sheet-like structures. The average particle size is about 15 nm. The size of all the CuS nanoparticles is smaller than most of the solar spectrum's range. According to Mie scattering theory^[21], scattering effects become negligible when the particle size is smaller than 1/20 of the incident wavelength. This characteristic ensures that the nanofluid primarily exhibits absorption/transmission behaviors rather than detrimental light scattering across the solar spectrum, which is crucial for achieving precise spectral splitting. The suppressed scattering losses enable accurate control over photon management, allowing optimal spectral allocation between photovoltaic and photothermal conversion components. What is more, the nanoscale homogeneous dispersion system effectively prevents optical performance degradation induced by particle agglomeration, ensuring long-term stability of the spectral splitting fluid.

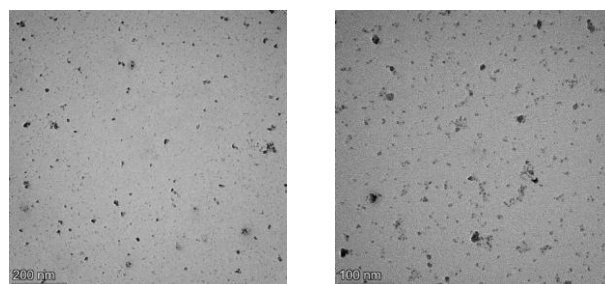


Figure 4. TEM image of Sample 1 CuS₂₅ nanoparticles

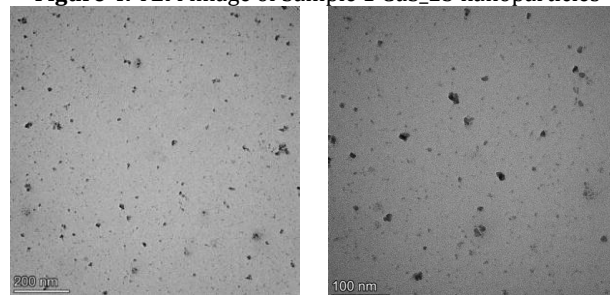


Figure 5. TEM image of Sample 2 CuS₄₀ nanoparticles

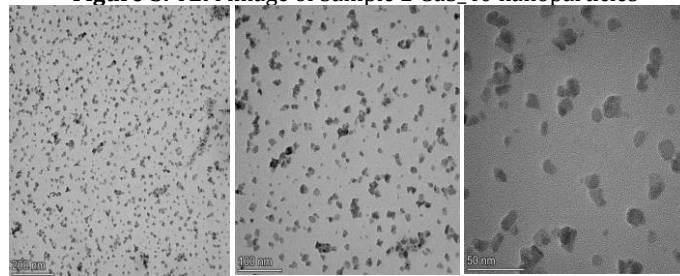


Figure 6. TEM image of Sample 3 CuS₆₀ nanoparticles

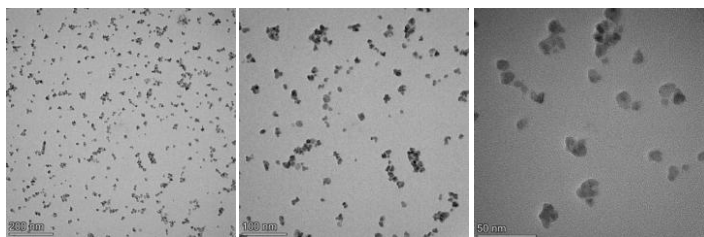


Figure 7. TEM image of Sample 4 CuS₈₀ nanoparticles

Figure 8 shows the XRD of sample 1, sample 2, sample 3, and sample 4 CuS nanoparticles. The structural characterization of the prepared samples was conducted using an X-ray powder diffractometer, and the results are shown in figure 8. The diffraction pattern indicates that the characteristic peaks of the prepared CuS₂₅, CuS₄₀, CuS₆₀, and CuS₈₀ samples match the standard card (PDF#06-0464). X-ray diffraction analysis confirms that all samples exhibit a pure hexagonal covellite phase (PDF#06-0464), with characteristic (102), (103), and (110) planes corresponding to diffraction peaks at 29.12°, 31.92°, and 48.27°, respectively. This well-defined crystalline purity ensures a stable optical bandgap and predictable photothermal conversion properties. The observed enhancement in diffraction peak intensity and sharpening of peak profiles with increasing reaction temperature indicates improved crystallinity, which facilitates charge carrier mobility and enhances photothermal conversion efficiency. Notably, the predominant development of (103) crystallographic planes strengthens surface plasmon resonance effects, enabling selective near-infrared absorption while maintaining visible light transmittance—a crucial feature for efficient solar spectral splitting. When combined with the nanosheet morphology (~15 nm) revealed by TEM characterization, the CuS nanofluid demonstrates exceptional spectral modulation capabilities, offering an optimal solution for photovoltaic-thermal hybrid systems through precisely controlled photon management.

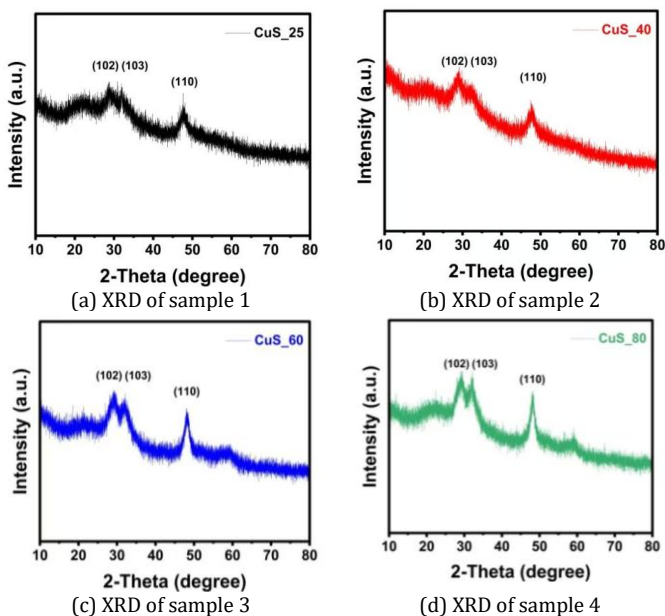


Figure 8. XRD pattern of CuS nanoparticles

3.2. The transmittance of the CuS Nanofluid

The transmittance of CuS nanofluid with both optical thickness of 10 mm were measured. The measured results are shown in figure 9 to figure 12.

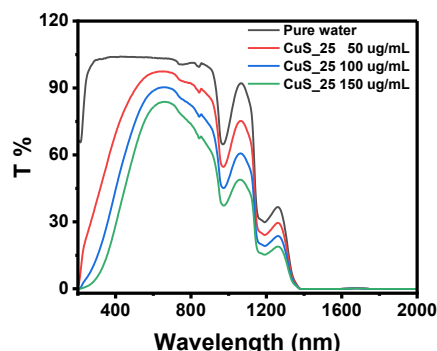


Figure 9. The transmittance of sample 1 CuS₂₅ nanofluid with three concentrations

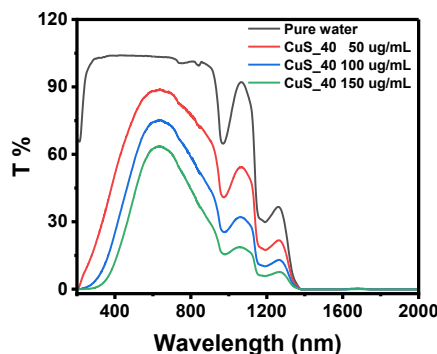


Figure 10. The transmittance of sample 2 CuS₄₀ nanofluid with three concentrations

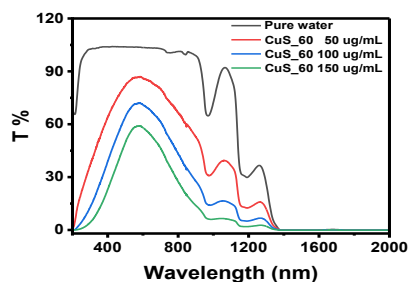


Figure 11. The transmittance of sample 3 CuS₆₀ nanofluid with three concentrations

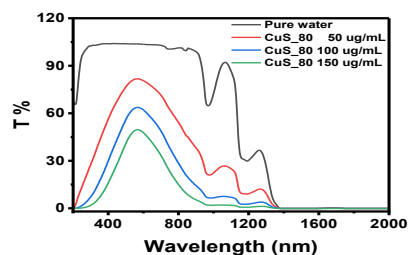


Figure 12. The transmittance of sample 4 CuS₈₀ nanofluid with three concentrations

As shown in Figure 9, the transmittance of sample 1 CuS₂₅ nanofluid is represented. Referring to figure 1, it can be seen that the ideal nanofluid should have high transmission characteristics in the 300nm to 1050nm band, while in the band less than 300nm or greater than 1050nm the fluid should have a strong absorption effect. According to Figure 9, the transmittance decreases with the increase in CuS nanofluid concentration. When the concentration of Sample 1 is 50 µg/ml, the average transmittance is at its maximum compared to the sample of 100 µg/ml and the sample of 150 µg/ml. At 600 nm, the transmittance reaches its peak, approximately 95 %. Although CuS₂₅ nanofluid exhibits high transmittance in the visible light range, it still maintains elevated transmittance between 1050 nm and 1300 nm. At the wavelengths of 1100 nm and 1250 nm, the transmittance of water has two obvious peaks. For CuS nanofluids, those peaks still exist. At 1100 nm, the transmittance is approximately 90%, while at 1250 nm, it is around 40 %. This behavior does not meet the requirements for spectral splitting nanofluids in PV/T systems. Therefore, the sample 1 CuS₂₅ nanofluid cannot be used in the spectral splitting PV/T system. Further research on the synthesis of CuS nanofluid has been implemented.

As the temperature of the oil bath rises, the transmittance of CuS nanofluid in the near-infrared wavelength range decreases. When the oil bath temperature reaches 80 °C, the decrease in transmittance of CuS nanofluid in the near-infrared wavelength range becomes significant. As shown in figure 12, the transmittance of sample 4 CuS₈₀ nanofluid is represented. It can be seen that the transmittance also decreases with the increase in CuS nanofluid concentration. The transmittance of sample 4 CuS₈₀ nanofluid with the concentration of 50 ug/ml is maximum compared to sample 4 of CuS nanofluid with the concentration of 100 ug/ml and sample 4 CuS₈₀ nanofluid with the concentration of 150 ug/ml. Although there are still two peaks at the wavelengths of 1100 nm and 1250 nm, the transmittance of sample 4 significantly decreases compared to the other three samples and water. The transmittance of sample 4 with the concentration of 50 ug/ml at the wavelength of 1100 nm is lower than 30 %, while the transmittance of sample 1 with the same concentration is 75 %. The transmittance of sample 4 has decreased by 45 %. The transmittance of sample 4 at the wavelength of 1250 nm is lower than 15 %, while the transmittance of sample 1 is 40 %. The transmittance of sample 4 has decreased by 25 %. For the sample 4 with the concentration of 100 ug/ml and the concentration of 150 ug/ml, the two peaks at the wavelengths of 1100 nm and 1250 nm almost disappear, which means that the transmittance of sample 4 in the wavelengths of the near-infrared range and infrared range can be effectively reduced. At the same time, the transmittance of sample 4 in the visible light range is still sufficiently high. The transmittance of sample 4 at the wavelength of 600 nm can hit 85 %. It means that CuS₈₀ exhibits significantly enhanced near-infrared absorption while maintaining high visible-light transmittance. This exceptional spectral

selectivity originates from the temperature-induced particle maturation effect. Combined XRD and TEM characterization reveals that elevated synthesis temperature not only increases nanoparticle size (thereby extending the photon transmission path) but also improves crystallinity, synergistically enhancing near-infrared photon harvesting. Notably, the CuS₈₀ nanofluid at an optimized concentration of 100 µg/mL displays ideal spectral-splitting performance—with near-infrared characteristic peaks almost completely diminished (transmittance <16 % at 1100 nm) while maintaining considerable visible-light transmittance (~65 % at 600 nm), perfectly fulfilling the critical "visible-transparent/near-infrared-absorbent" requirement for PV/T hybrid systems. This spectrally tailored strategy, achieved through precise control of synthesis temperature (80 °C) and concentration optimization (100 µg/mL), provides an important material solution for designing high-efficiency solar spectral splitting systems.

In comparison with other nanofluids, the CuS₈₀ nanofluid demonstrates superior spectral modulation capabilities, particularly exhibiting enhanced selective absorption in the near-infrared region while maintaining high visible light transmittance. When benchmarked against silver-based nanofluids, CuS₈₀ presents remarkable cost advantages, with raw material costs representing merely 3% of those required for Ag-based systems, thereby significantly improving economic viability for large-scale implementation. Relative to polypyrrole nanofluids, CuS₈₀ displays exceptional photochemical stability under prolonged operational conditions. These outstanding properties collectively establish CuS nanofluids as an ideal candidate for solar spectral splitting applications.

3.3. The Reflectivity of the CuS Nanofluid

Figure 13 shows the reflectivity of sample 4 CuS₈₀ nanofluid. The reflectivities of three concentrations have the same trend, which decreases with the increase of wavelength. Between the wavelength range of 200 nm and 230 nm, the reflectivity exhibits significant fluctuations. In the range of 230 nm to 500 nm, the reflectivity decreases sharply from 20 % to 4 %. From 500 nm to 1400 nm, the rate of decrease in reflectivity slows down, dropping from 4 % to 1 %. Finally, in the wavelength range of 1400 nm to 2000 nm, the reflectivity fluctuates again.

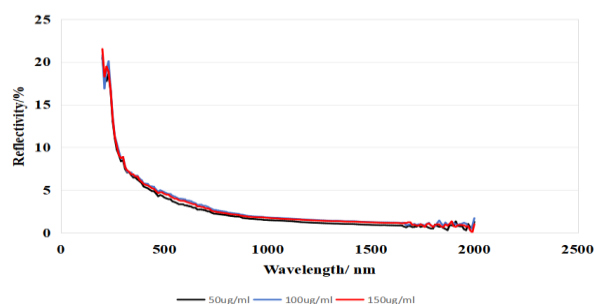


Figure 13. The reflectivity of sample 4 of CuS₈₀ nanofluid with different concentrations

4. CONCLUSION

The optical properties of CuS nanofluid for the spectral splitting PV/T system have been successfully observed and evaluated. The sample 4 CuS_80 exhibits a well-selective absorption characteristic whose average size is 15 nm. When the concentration is 100 ug/ml, the optical characteristic is best. The transmittance near the visible band of sample 4 CuS_80_100 ug/ml is high, while that in the near-infrared band is low. The high absorptance offers a good condition for improving the temperature of photothermal in the PV/T system. Therefore, these optical properties provide strong support for the wide application of CuS nanofluid in the spectral splitting PV/T system.

ACKNOWLEDGMENTS

This research was funded by 3 grants from the Nantong Municipal Science and Technology Plan Project on Social Livelihood (MSZ2023001) and the Natural Science Foundation of the Jiangsu Higher Education Institutions of China (23KJB460009; 23KJB470006).

REFERENCES

- [1] Y. Jiao, M. Xing, and P. Estellé, "Efficient utilization of hybrid photovoltaic/thermal solar systems by nanofluid-based spectral beam splitting: A review," *Solar Energy Materials and Solar Cells*, vol. 265, p. 112648, 2024.
- [2] M. R. Fernandes and L. A. Schaefer, "Multiparticle nanofluid optimization for spectral-splitting energy harvesting," *Renewable Energy*, vol. 173, pp. 849–860, 2021.
- [3] G. Zhang, S. Shan, H. Wu, et al., "Investigation on the radiative characteristics of ZnO-SiO₂ nanofluids in spectral splitting photovoltaic/thermal systems," *Solar Energy Materials and Solar Cells*, vol. 277, p. 113129, 2024.
- [4] X. Han, X. Zhao, J. Huang, et al., "Optical properties optimization of plasmonic nanofluid to enhance the performance of spectral splitting photovoltaic/thermal systems," *Renewable Energy*, vol. 188, pp. 573–587, 2022.
- [5] W. An, et al., "Experimental investigation of a concentrating PV/T collector with Cu₉S₅ nanofluid spectral splitting filter," *Applied Energy*, vol. 184, pp. 197–206, 2016.
- [6] G. Yu, L. Dai, and G. Gu, "Analysis of energy performance of nanofluid-based spectral splitting photovoltaic/thermal collectors of different designs," *Applied Solar Energy*, vol. 59, no. 3, pp. 253–268, 2023.
- [7] Y. Xiao, W. Tian, L. Yu, et al., "Tunable optical properties of ATO-CuO hybrid nanofluids and the application as spectral beam splitters," *Energy*, vol. 289, p. 129964, 2024.
- [8] H. Liang, X. Huang, F. Wang, et al., "Multiple nanoparticles coupling strategy for enhancing optical filter performance of spectral splitter used in photovoltaic/thermal system," *Journal of Thermal Science*, vol. 33, no. 1, pp. 368–382, 2024.
- [9] B. Yang, Y. Zhi, Y. Qi, et al., "Advancing performance assessment of a spectral beam splitting hybrid PV/T system with water-based SiO₂ nanofluid," *Frontiers in Energy*, pp. 1–17, 2024.
- [10] J. Guan, J. Sun, X. Shi, et al., "Review of full-spectrum solar energy systems based on spectral splitting technology," *International Journal of Hydrogen Energy*, vol. 81, pp. 1235–1255, 2024.
- [11] X. Xia, W. Wei, B. Yu, et al., "Experiment and numerical investigation on a spectral splitting PV/T system for electrical energy and thermal output," *Energy*, vol. 288, p. 129911, 2024.
- [12] Y. Jiao, M. Xing, and P. Estellé, "Efficient utilization of hybrid photovoltaic/thermal solar systems by nanofluid-based spectral beam splitting: A review," *Solar Energy Materials and Solar Cells*, vol. 265, p. 112648, 2024.
- [13] G. Zhang, S. Shan, H. Wu, et al., "Investigation on the radiative characteristics of ZnO-SiO₂ nanofluids in spectral splitting photovoltaic/thermal systems," *Solar Energy Materials and Solar Cells*, vol. 277, p. 113129, 2024.
- [14] X. Xia, X. Cao, N. Li, et al., "Study on a spectral splitting photovoltaic/thermal system based on CNT/Ag mixed nanofluids," *Energy*, vol. 271, p. 127093, 2023.
- [15] L. Huaxu, W. Fuqiang, Z. Dong, et al., "Experimental investigation of cost-effective ZnO nanofluid based spectral splitting CPV/T system," *Energy*, vol. 194, p. 116913, 2020.
- [16] L. Huaxu, W. Fuqiang, L. Dong, et al., "Optical properties and transmittances of ZnO-containing nanofluids in spectral splitting photovoltaic/thermal systems," *International Journal of Heat and Mass Transfer*, vol. 128, pp. 668–678, 2019.
- [17] M. U. Sajid and Y. Bicer, "Nanofluids as solar spectrum splitters: a critical review," *Solar Energy*, vol. 207, pp. 974–1001, 2020.
- [18] X. Han, X. Zhao, J. Huang, et al., "Optical properties optimization of plasmonic nanofluid to enhance the performance of spectral splitting photovoltaic/thermal systems," *Renewable Energy*, vol. 188, pp. 573–587, 2022.
- [19] D. Majumdar, "Recent progress in copper sulfide based nanomaterials for high energy supercapacitor applications," *Journal of Electroanalytical Chemistry*, vol. 880, p. 114825, 2021.
- [20] Z. Huang, L. Wang, H. Wu, et al., "Shape-controlled synthesis of CuS as a Fenton-like photocatalyst with high catalytic performance and stability," *Journal of Alloys and Compounds*, vol. 896, p. 163045, 2022.
- [21] Y. A. Akimov, "Mie scattering theory: a review of physical features and limitations," *arXiv preprint*, arXiv:2401.04146, 2024.